Design and development of a miniaturized scanning probe

L.M. Wurster, W.C. Warger, M.J. Gora, R. Carruth, G.J. Tearney, R. Birngruber

This paper presents the design of a scanning probe based on a dual-wedge scanner concept. In contrast to the original dual-wedge scanner, which consisted of two prisms, this scanner utilizes one prism and an angle-polished ball lens to reduce the total size. By separately rotating the ball lens and prism at different speeds, it is possible to achieve a two-dimensional spiral or rosette scan pattern. The advantage of this scanning probe is its potential to be miniaturized. The scanner presented here has a cylindrical diameter of 3.9mm and a length of 4mm, allowing applications of imaging inner organs *in vivo*.

I. Introduction

Point-scanning optical imaging techniques such as optical coherence tomography (OCT) or confocal microscopy require a scanning system where information from each position within the image is acquired separately. A scanning system generally works by continuously tilting the direction of the light beam in the back focal plane of the objective lens to translate the beam to different points within the field of view (FOV). The standard scanner, consisting of two mirrors to scan uniformly throughout the FOV in the x and y directions, adds size to the system. Alternative smaller scanning probes have been developed, and can be divided into two categories: forward-imaging and side-imaging systems. The smallest reported side-imaging probe has an outer diameter of 0.4mm and produces a helical scan by rotating the probe and translating in the axial direction to generate a 3D image [1]. It is important to note that side-imaging devices are typically limited to imaging cylindrical geometries, making the technique ideal for image vessels, but suboptimal for other geometries. Forward imaging probes are more difficult to miniaturize because a complex system is required to provide accurate and reproducible translation within the axial direction. The narrowest forward imaging probe is 0.82mm in diameter, but has been designed as an optical coherence tomography needle endoscope being relatively long and rigid [2]. Another interesting small forward imaging probe with a diameter of 1.2mm and a length of 9mm is the scanning fiber endoscope that uses a single fiber to create a spiral scan [3]. An alternative method for scanning the beam in the forward direction is a dual-wedge scanner. The first description of a dual-wedge scanner was Rosell in 1960, under the name Prism scanner [4]. Since then, a dual-wedge scanner has been used in different configurations; including the dual-wedge scanner for laser radar system [5], the Risley prism scanner [6], and the pair-angle rotation scanner for aforementioned OCT needle probe [2].

The aim of this project is to build a small scanning device with an overall size that is approximately 4mm in diameter by 4mm in length with the use of a dual-wedge scanning system consisting of an angle-polished ball lens and a prism. This device overcomes challenges associated with very small lateral or axial movements by using the simplicity of the mechanical rotation. To the best of our knowledge, this device has the smallest volume of any forward imaging scanning probe reported to date. We have designed the probe to connect it to an OCT system, but in general it could be combined with any optical imaging system that requires a two-dimensional forward scanning system. The required parameters, when working with the probe and the 1310nm broadband laser source of the OCT system are a focus spot size of 30µm, working distance of ~2.5mm and a FOV with a radius of 0.72mm.

II. Material and Methods

A. Scanning concept

The dual-wedge scanning concept is shown in Fig.1. The prism is oriented such that the first surface is perpendicular to the optical axis and deviates the beam by the deviation angle θ. By rotating the prism about the optical axis, the light beam scans a circle with radius *v*1. Adding a second prism with the same deviation angle (*v*1=*v*2) or in this case an angle-polished ball lens, causes the beam to deviate by *v*1+*v*2. If the prism is held stationary and the ball lens is rotated around 360 degree a

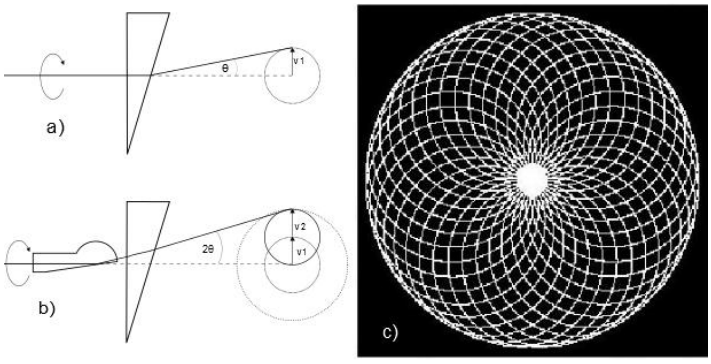

Fig. 1 Scanning concept a) a single prism deviates the beam by the vector *v*1, by rotating the prism a circle is scanned b) by placing a ball lens in front of the prism the beam gets deviated by 2θ c) Rosette scan pattern

L.M. Wurster, Medizinische Ingenieurwissenschaft, University of Luebeck; the work has been carried out at the Wellman Center for Photomedicine, Massachussetts General Hospital, Harvard Medical School, Boston, USA (tel.: +1-617-949-1871,e-mail: lwurster@partners.org), W.C.Warger (tel.:+1- 617-643-2894, e-mail:wwarger@gmail.com), M.J. Gora (tel.:+1-617-643-9209, e-mail:mgora@partners.org), R. Carruth (tel.+1-617-643-9227,e-mail: pcarruth@partners.org) G. J. Tearney (tel. +1-617-724-2979, e-mail: tearney@helix.mgh.harvard.edu) are with Wellman Center for Photomedicine, Massachusetts General Hospital, Harvard Medical School, Boston, USA
R.Birngruber,(tel.+49-451-500-6504,e-mail:bgb@bmo.uni-luebeck.de) is with University of Luebeck, Insititute for Biomedical optics, Luebeck, Germany

circle with radius *v*2 is scanned as shown in Figure 1b. By rotating both elements about the optical axis in the same direction with slightly different speeds a spiral scan can be produced. Rotating the prisms in opposite directions with one element rotating much faster than the other creates a rosette scan, such as that shown in Figure 1c [4]. Various scan patterns can be generated, depending on the relation of the rotation speeds and their directions [5]. It is important to note that the deviation angle of the prism and the angle of the polished ball lens must be the same (*v*1=*v*2) or a region in the middle of the image will not be scanned [7].

The disadvantage of this type of scan pattern is that it requires a sophisticated image reconstruction method that remaps the spiral scan pattern into Cartesian coordinates. These mapping algorithms typically calculate the exact location of each spot within the FOV based on the knowledge of the rotation angle of the prisms. Precise knowledge of the rotation angles can be accomplished using position feedback encoders that are associated with the motors that turn the prism and the ball lens.

B. Ray tracing

Zemax is a ray-tracing software that is commonly used in research and industry to design and analyze optical systems. The software provides two modes of light-propagation: standard sequential ray tracing and non-sequential ray tracing. The sequential mode provides a variety of tools for optimization and analysis of optical properties, where each optical element is defined by the individual surfaces the light propagates through (curvature, reflectivity, tilt, etc.). The rays are incident at each surface in the order in which the surfaces are defined, from the source, through each object surface, until reaching the last image surface. For our design, the sequential mode was used to optimize the ball lens for an adequate focal spot size and working distance between the output of the ball lens and the imaged FOV. In non-sequential ray tracing there is no pre-defined path for any ray such that optical components can be modeled as true three-dimensional objects and placed at independent coordinates. Using this mode the ball lens and the prism can be rotated to simulate the resultant scan pattern.

C. Design of the scanning probe

Fig. 2 shows the design of the imaging system that we used to test the proposed optical scanning probe. The probe is designed to function in the sample arm of an optical frequency domain imaging (OFDI) system [8]. OFDI is a second-generation form of OCT that provides depth-resolved images at very high speeds and is also known as swept-source Fourier Domain OCT. Near-infrared light (1310nm) is delivered to and collected from the tissue by means of an optical fiber terminated with the dual-wedge. In order to use the probe for biomedical applications, the length of probe must be adequate to extend from the OFDI system, through the body, and into the imaged organ. Based on our group's previous work with the biomedical imaging, we chose a probe length of 1.6m. To

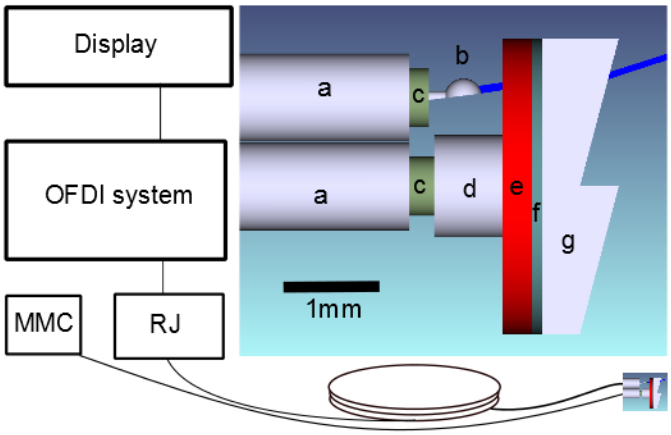

Fig. 2 Design of the scanning probe, the connections to the motors and the OFDI system, a) sheath, b) fiber with ball lens, c) drive shaft, d) acrylic collar, e) acrylic disc, f) epoxy, g) Fresnel prism

rotate the fiber and ball lens (Fig.2b) over this length, the fiber is enclosed a 0.6mm three layer torque coil (driveshaft) (Fig. 2c) within a 0.85mm outer sheathing to provide torque delivery from the proximal end of the catheter to the distal tip. The prism (Fig. 2g) is rotated using a separate driveshaft (Fig. 2c) and sheath to ensure the wedged surfaces rotate independently. At the proximal end of the probe, both driveshafts are attached to separate motors (optical rotary junction (Fig. 2 RJ) for the ball lens and Maxon hollow shaft motor (Fig. 2 MMC) for the prism). To rotate the prism with minimal wobble, an acrylic disc (Fig. 2e) was secured to the prism with epoxy, which was then epoxied to an acrylic collar (Fig.2d) to connect the driveshaft. It is important to note that the flat prism wall must be perpendicular to the axis of the driveshaft. As such a separate holder was machined to hold all of the components at the right orientation while the epoxy cured.

D. Fresnel prism

One concern with regard to the spinning mechanism was that a standard prism would not be mechanically balanced and therefore would wobble when rotated. As a result, we decided to utilize a so-called "Fresnel prism", which is an array of multiple small prisms within a sheet. The advantage of the Fresnel prism is that the use of multiple smaller prisms makes it thinner and distributes the weight more equally over the optical element. A single prism of the Fresnel prism used for the first prototype has a width of 1.5mm. The Fresnel prism provided 12 diopters of deviation, where diopters are defined as the deflection of the light by 1cm at a distance of 1m from the prism [9]. Therefore, the optical deviation angle was 6.89, without considering the index of refraction of the material. To more accurately compute the refraction angle, an OFDI image of the prism was acquired to calculate the wedge angle and the refractive index of the material at 1310nm [10]. With a measure refractive index of 1.548 and a wedge angle of 14.82 degree (in air), we calculated that the Fresnel prism would refract the beam by 8.5 degrees.

E. Ball lens

Ball lenses are typically used for coupling light between fibers because of their short focal lengths, but are also used as lenses to focus or collimate light. In order to provide adequate focusing of the beam, it is necessary to provide some distance between the tip of the fiber core and the focusing surface of the ball lens for the light beam to expand. This distance is created by splicing a spacer with a similar diameter and homogeneous index of refraction between the fiber tip and the ball lens. To simplify the assembly, the ball lens was also created by the same spacer material. Once the ball was created, the ball lens was polished at a specific angle such that the light was reflected by total internal reflection at the desired deviation angle. This approach is often used for side imaging probes-, by using a polishing angle around 45 degrees.

The ball lens was produced using an all-in-one fiber-optic fusion splicing station from Vytran (FFS-2000) that uses localized heat to melt or fuse the fiber ends. The process began by fusing the fiber spacer (coreless fiber) and a SMF-28 fiber. Both fibers were stripped of their protective coatings and cleaved to cut the fiber perfectly flat and perpendicular to the optical axis. A small tungsten filament in the fusion splicer then heated the two fiber tips and melted the fibers together. Once the fibers were spliced, an adequate amount of spacer material was cleaved onto the end of the fiber to provide the desired spacer length and ball diameter. The ball lens was then produced by using the filament again to melt the coreless fiber. Various ball sizes can be produced by modifying user defined fusion splicer's software macros, which control how fast the fiber moves to the filament, the power of the filament and the time of the melting process. With this fusion splicer system the largest radius ball lens that could be achieved was approximately 200µm.

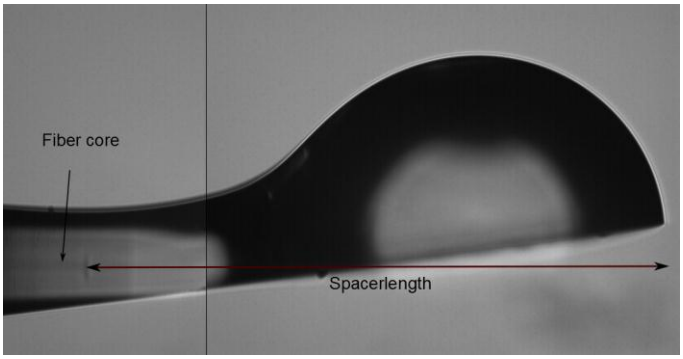

Fig 3 Photograph of a ball lens, polished with a 7.8 degree angle and a spacer length of 605µm

As mentioned previously it is possible to use the ball lens as focusing element depending on the length of the spacer and the curvature of the ball. With no spacer, the light will diverge out of the ball. As the spacer length increases, the divergence of the light will decrease until the beam is eventually collimated. After that point, further lengthening of the spacer will focus the beam.

Polishing the ball lens so that the light beam exits the surface of the ball lens perpendicular to the surface has no influence on the light beam, including the focal spot. In our case, however, the polishing angle was very small, because we needed to match the small deviation angle of the prism. That causes that the light exits the curvature of the ball lens at an angle not perpendicular to the surface, what results in optical aberrations that changes the location and size of the focal spot, which also have to be taken into account.

Once the ball lens was created with the desired spacer length the ball was polished at the desired angle with a fiber-optic polisher (Ultrapol Fiber Lensing Machine). A polished ball lens with a 605µm spacer length is shown in Fig. 3. It is important to note that the FOV of the fusion-splicer's camera was too small to image the fibercore and the ball lens in one picture; therefore, two images were merged together to create the figure.

III. Results and Discussion

A. Ray tracing

Zemax modeling provided the expected results with an ideal spacer length, ball lens diameter, polish angle, and the influence of the ball lens position. However, it was not possible to predict the exact probe parameters due to the difficulties in simulating the errors that occurred during the fabrication. The design was sensitive with a tolerance of 10µm with regard to the spacer length, ball lens radius and polishing position. As a result, a variety of ball lenses and spacer length configurations were produced and the spot size was measured (see part B). As mentioned previously, the polished angle of the ball lens must match the deviation of the prism, and Zemax was used to determine that a 7 degree angle-polished surface will deviate the beam by 8.5 degrees.

B. Measured results

TABLE I
CHARACTERIZATION OF DIFFERENT POLISHED BALL LENSES

Parameter	Ball 1	Ball 2	Ball 3	Ball 4
Spacer (µm)	565	605	620	640
Radius-y (µm)	187	185	185	186
Radius-x (µm)	201	199	202	200
Angle (degree)	7.06	7.8	7.19	5.6

TABLE II
SPOT SIZE OF DIFFERENT BALL LENSES

	Spot size diameter (µm)			
Distance (mm)	Ball 1	Ball 2	Ball 3	Ball 4
0*	45	48	63	50
0.5	44	48	63	40
1	46	49	62	40
1.5	52	54	66	45
2	65	59	53	45
2.5	71	62	59	50
3	78	67	74	57
3.5	86	72	80	66
4	95	78	87	76
4.5	102	84	96	84
5	112	91	98	97

*assuming that the distance between ball lens and detector is close to 0

Table I shows the spacer lengths, sizes and polished angles of the ball lenses. The spot size and working distance of the fabricated ball lenses were measured with a CCD camera (WinCamD UCD12-1310) to visualize the 1310nm OFDI beam. The results are shown in Table II. The focal spot size was measured as the full-width-at-half-maximum of the beam. Measurements were recorded along orthogonal directions and averaged. As expected, due to the aberration caused by the angle at which the light exits the ball lens, the beam shape observed during measurements, was not perfectly Gaussian.

The production process of the ball lens was quite difficult because the final spacer length was not predictable and could vary by ± 150µm. Furthermore the polished angle slightly changed and it was not possible to polish a ball lens with exactly the desired 7 degree angle (see Table I). The size of the ball lens, however, was relatively reproducible with differences of only a few µm (see Table I).

C. Resulting probe and Scan pattern

Fig. 4 shows a photograph of the probe, assembled using Ball lens 1. The prism was mounted in a brass tube. The brass tube containing the prism was then rotated inside of a separate, outer brass tube. Brass was used because of its ease to machine but for medical applications it will be replaced by a USP class VI polymer.

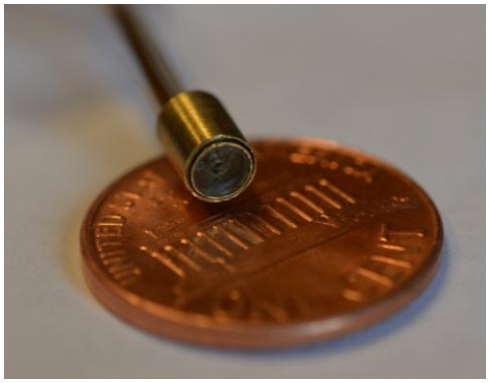

Fig. 4 Photograph of the probe with a penny as scale

Fig. 5 shows a scan pattern that was achieved with this device. In order to create this scan pattern, we rotated the ball lens at 600rpm and the prism at 3600rpm. These speeds were chosen to provide a visual clear representation of the scan pattern. In order to achieve greater sampling of the two-dimensional area, we will need to increase the differences between the two rotational velocities. It is also important to note that a small region within the center of the scan pattern was not sampled due to the ball lens having an optical deflection angle that was different from that of the prism. This can be mitigated in the future by attaining higher tolerance on the polishing angle of the ball lens.

Finally, in order to create an image from the scan pattern, the Cartesian coordinates of the image must be determined from a precise knowledge of the rotational angles of each prism. This data may be obtained by use of position feedback encoders on the motors.

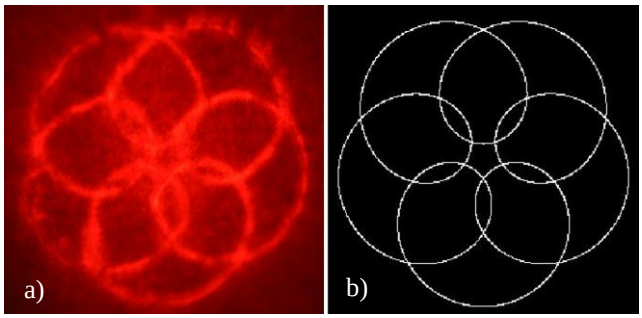

Fig. 5 Rosette scan pattern, a) Photograph of a scan pattern achieved by using the probe, b) simulated scan pattern for the known rotational speeds and diffraction angles of light transmitted by the polished ball lens and prism

IV. CONCLUSIONS

This paper presents a proof-of-principle design and preliminary testing of a miniaturized dual-wedge scanning probe. Our results demonstrate that a very small beam scanner can be created and can provide a rosette scan pattern in accordance with simulations. In order to make the probe fully functional, we will need to change the motor speeds, polish the ball lens more accurately, and obtain feedback regarding the instantaneous angles of both prisms to remap the image coordinates.

ACKNOWLEDGEMENTS

We would like to thank Paulino Vacas Jacques, Ali M. Fard, and Hao Wang who assisted with the construction of the ball lenses and have been a great source of expertise.

REFERENCES

[1] X.D.Li, C.Chuboda, T.Ko, C.Pitris, J.G.Fujimoto, "Imaging needle for optical coherence tomography," *Optics Letters*, vol. 25, no. 20, pp. 1520-1522, 2000.

[2] S.Han, M.V.Sarunic, J.Wu, M.Humayun, C.Yang, "Handheld forward-imaging needle endoscope for ophthalmic optical coherence tomography inspection", *Journal of Biomedical Optics*, vol.13, no 2, 2008

[3] E.J.Seibel, R.S. Kohnston, C.D. Melville, "A full-color scanning fiber endoscope", *Proc. SPIE 6083*, 2006

[4] F.A.Rosell, "Prism scanner" *J.Opt.Soc.Am.*, vol. 50, no. 6, pp.521-526, June, 1960

[5] C.T. Amirault, C.A. DiMarzio, "Precision Pointing Using a Dual-Wedge Scanner", *Applied Optics*, vol. 24, pp.1302-1308, 1985

[6] G.F.Marshall, "Risley prism scan patterns" *Proc. SPIE* 3789, 1999

[7] W.C.Warger, C.A.DiMarzio, "Dual-wedge scanning confocal reflectance microscope," *Optics Letters*, vol. 32, no. 15, pp. 2140-2142, Aug. 2007.

[8] Yun, S.H., Tearney, G.J., de Boer, J.F., Iftimia, N. & Bouma, B.E." High-speed optical frequency-domain imaging," *Opt. Express*, vol 11, pp. 2953–2963, 2003

[9] M.Katz, Introduction to Geometrical Optics, Penumbra Publishing Co. Singapore, pp.58, 1994

[10] G.J.Tearney, "Determination of the refractive index of highly scattering human tissue by optical coherence tomography", *Optics Letters*, vol. 20, No. 21, pp.2258, 1995